

## Evaluation of rigid-end offset effect on seismic behavior of a structure subjected to Van earthquake

Serkan Bekiroğlu<sup>\*</sup>, Abdurrahman Şahin<sup>a</sup>, Barış Sevim<sup>a</sup> and Yusuf Ayyavaz<sup>b</sup>

*Yıldız Technical University, Department of Civil Engineering, 34220, Istanbul, Turkey*

*(Received March 5, 2013, Revised August 31, 2013, Accepted September 9, 2013)*

**Abstract.** Numerical damage assessment of Van train station building consisting of three RC blocks due to 2011 Van Earthquakes by nonlinear dynamic analysis is presented. The structural model is created with rigid-end offsets and plastic hinges for nonlinear analysis. Rigid-end offsets are considered for connection areas and proposed for wall-supported elements. In wall-supported elements, walls take place in a limited part of the columns. Nonlinear dynamic analysis of the building with and without rigid-end offsets is performed by using real earthquake records and results are compared. The results show that rigid-end offsets have significant effects on the seismic behavior of the structures.

**Keywords:** rigid-end offset; wall-supported elements; plastic hinge; nonlinear time history analysis

---

### 1. Introduction

A strong earthquake occurred on October 23, 2011 in Van located in the eastern part of Turkey. The magnitude of the earthquake is given 6.7 by the Earthquake Department of the Disaster and Emergency Management Presidency (AFAD). After this strong earthquake, one more earthquake with magnitude 5.6 occurred in nearly 10 km. South of Van City Center on November 9, 2011.

In Fig. 1, seismic hazard map created for Eastern Turkey by U.S. Geological Survey is presented. In this map, the peak ground accelerations distributions with 10% probability of exceedance in 50 years are given. The Van earthquake is signed with a big star in this map.

Earthquakes and their results give researchers opportunity to try theoretical developments on real structures. In this study, the structural behavior of the Van train station building subjected to the two major earthquakes is evaluated by nonlinear dynamic analyses with classical FE models and rigid end models. Rigid end model means that the connection areas and the element parts which are supported with walls are assumed as rigid.

Rigid-end offsets have been considered in some studies (Tsai *et al.* 1995, Khudada and Geschwindner 1997, Foley and Vinnakota 1999). The plastic hinge forming at locations offset from the rigid-end offset has been studied by Wong and Wang (Wong and Wang 2007a, b, Wong 2012). In this study, the importance of rigid-end offsets and wall-supported elements considering

---

\*Corresponding author, Assistant Professor, E-mail: serkanb@yildiz.edu.tr

<sup>a</sup>Associate Professor

<sup>b</sup>Professor

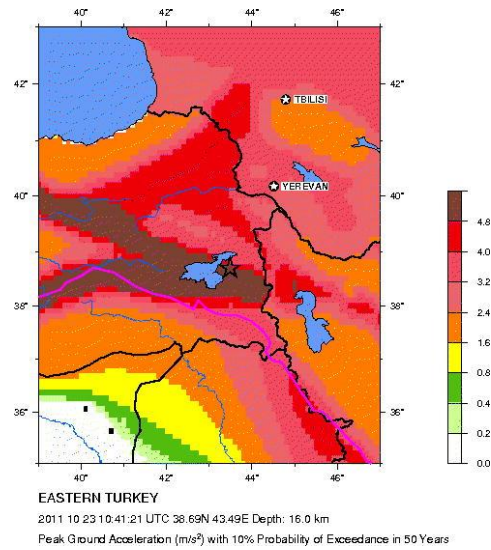


Fig. 1 Seismic hazard map for Eastern Turkey (Url-1)

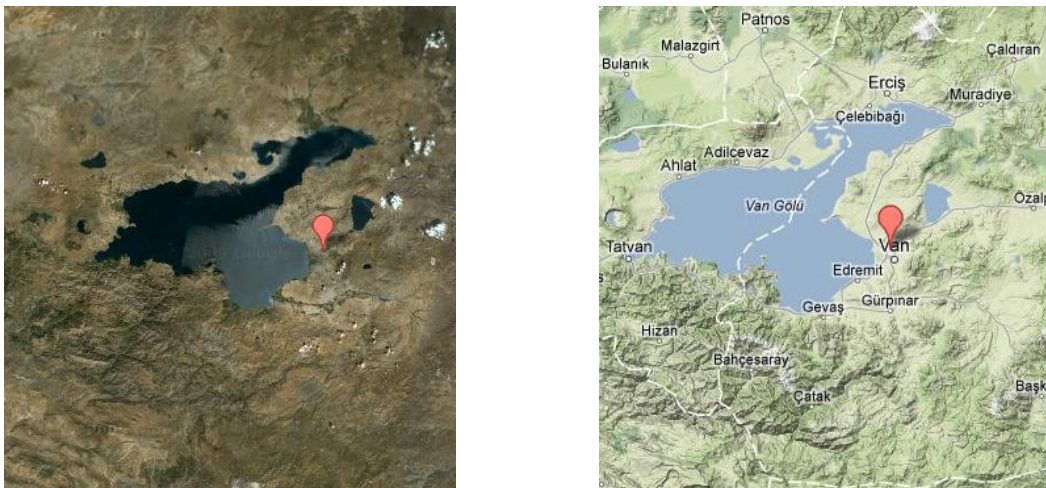


Fig. 2 Location of train station building in the map (Url-2)

plastic hinges is investigated on a real structure subjected to huge earthquakes in near time.

The location of the investigated train station building is presented in Fig. 2. As it can be seen from Figs. 1 and 2, the building is near to the center of the earthquakes.

## 2. Raw measured seismic records and spectrums

The first earthquake has magnitude 6.7 and has three components. These are north-south component, east-west component and up-down component as shown in Fig. 3.

The second earthquake has magnitude 5.6 and has three components. These are north-south component, east-west component and up-down component as shown in Fig. 4.

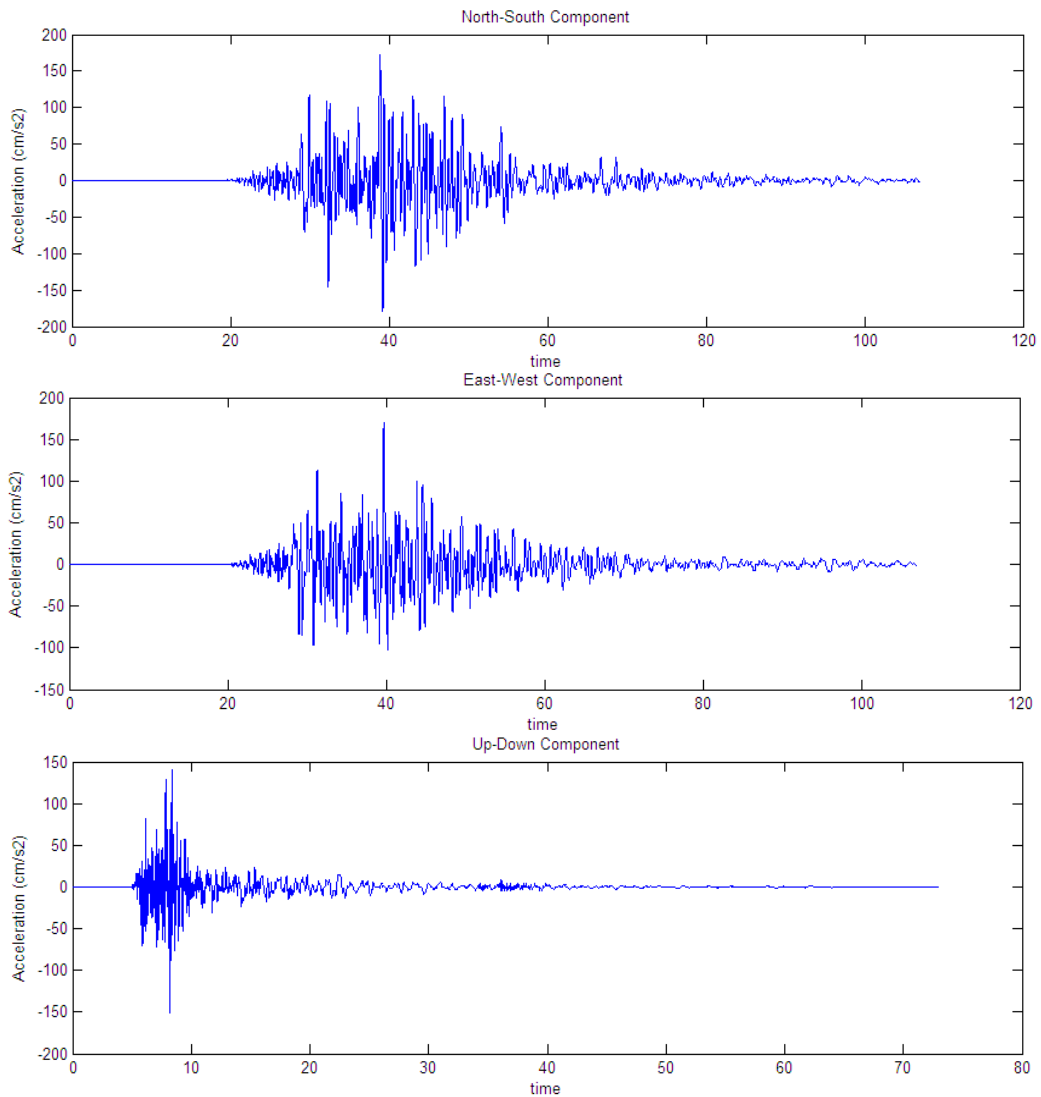


Fig. 3 Three components of the first earthquake with magnitude 6.7

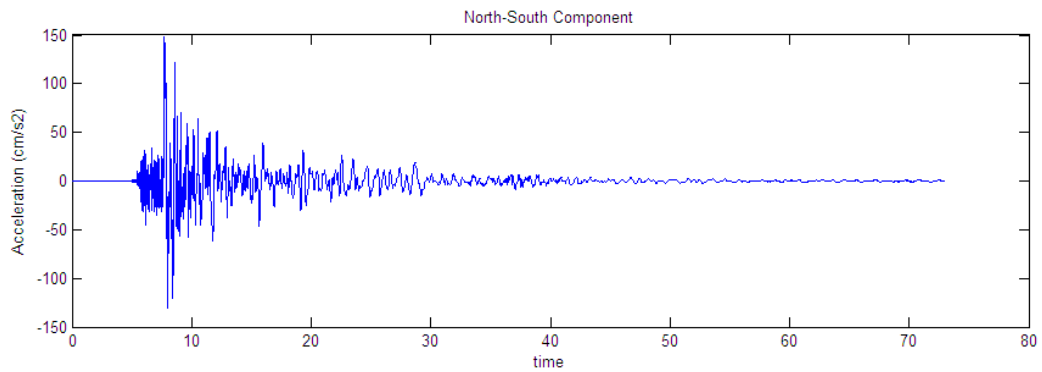


Fig. 4 Three components of the first earthquake with magnitude 5.6

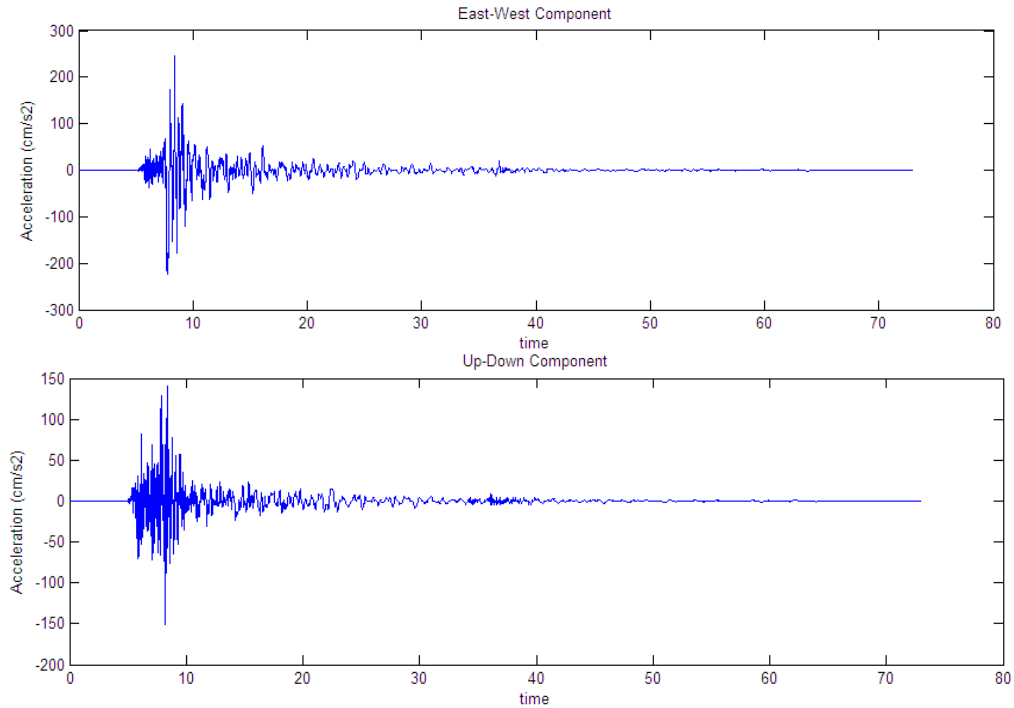


Fig. 4 Continued

To evaluate the soil behavior, spectral functions of the seismic record may be investigated. Autopower spectrums or power spectral densities give an idea about characteristic behavior of the soil.

### 3. Analyzing raw measured data and production of spectral functions

#### 3.1 Autospectrum analysis

The autospectrum of a time signal  $a(t)$  is given in Eq. (1) (Heylen *et al.* 2007)

$$G_{aa}(f) = A(f) \cdot A^*(f) \quad (1)$$

In Eq. (1),  $A(f)$  is the Fourier transform of  $a(t)$  and  $*$  indicates the complex conjugate. The autospectrum shows how the mean power in a signal is distributed over frequency. The autocorrelation function of a transient time signal  $a(t)$  is given in Eq. (2) (Heylen *et al.* 2007)

$$R_{aa}(\tau) = \int_{-\infty}^{+\infty} a(t) \cdot a(t + \tau) dt \quad (2)$$

For a stationary signal, the autocorrelation function is defined in Eq. (3)

$$R_{aa}(\tau) = \lim_{T \rightarrow \infty} \left( \frac{1}{T} \right) \int_{-T/2}^{T/2} a(t) \cdot a(t + \tau) dt \quad (3)$$

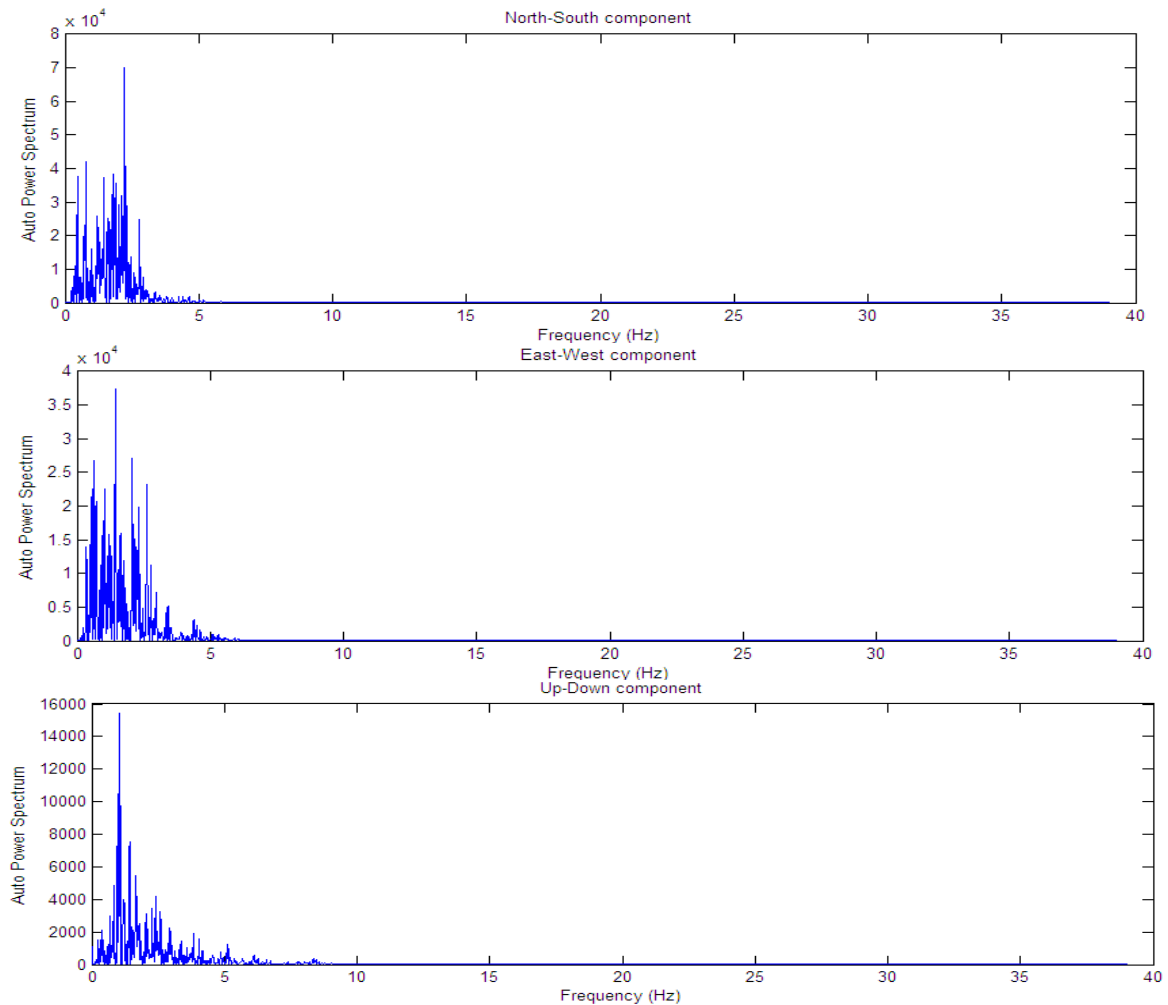


Fig. 5 The autospectrum graphics for all component of the first earthquake

The raw measured acceleration records are analyzed by using SignalCAD (Şahin and Bayraktar 2010) program developed in MATLAB (2009) and autospectrums are obtained. The calculated autospectrums by using rectangular window for the components of the first earthquake is presented in Fig. 5. The peak points of calculated spectrums are between 0.2 Hz and 7 Hz as it can be seen in this Fig. The spectrums of all components between these frequency intervals are given in Fig. 6.

The calculated autospectrums by using rectangular window for the components of the second earthquake is presented in Fig. 7. The peak points of calculated spectrums are between 0.2 Hz and 7 Hz as it can be seen in this Figure. The spectrums of all components between these frequency intervals are given in Fig. 8.

It can be understood from Figs. 5-8, the natural frequency of the soil system is between 0.2 Hz and 7 Hz. The structural response may be bigger between these frequency interval and if the natural frequencies of the soil and building coincide with each other, resonance risk must be taken into account.

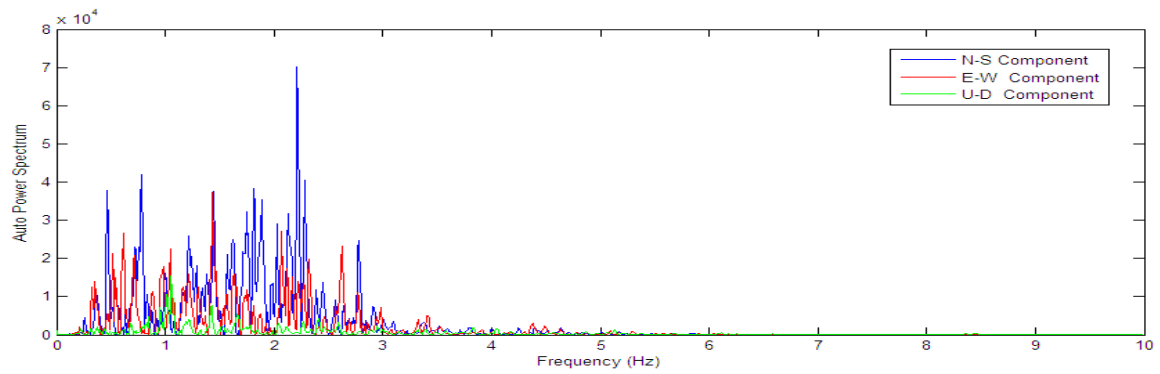


Fig. 6 The autospectrum graphics for all component of the first earthquake between 0-10 Hz

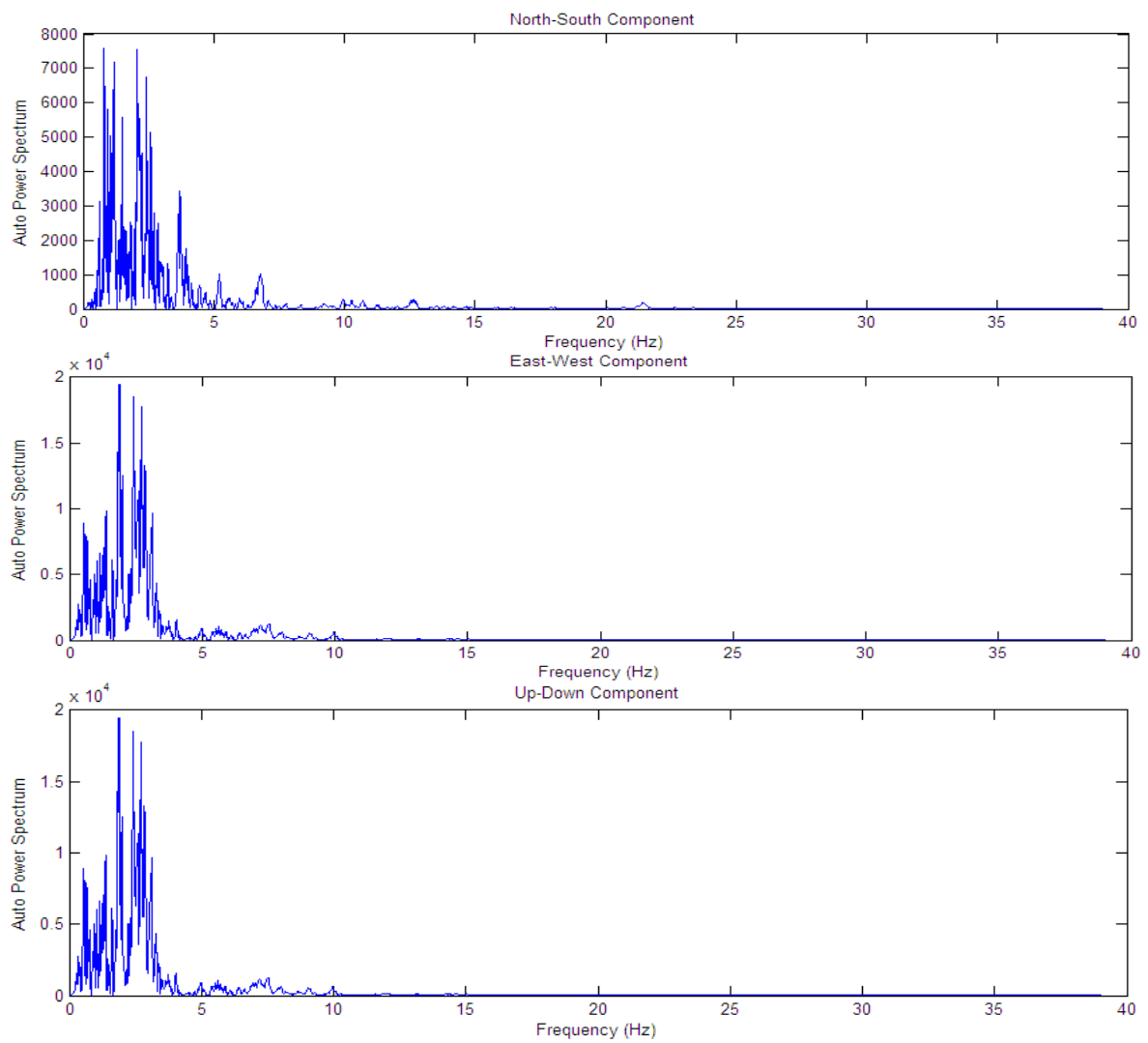


Fig. 7 The autospectrum graphics for all component of the second earthquake

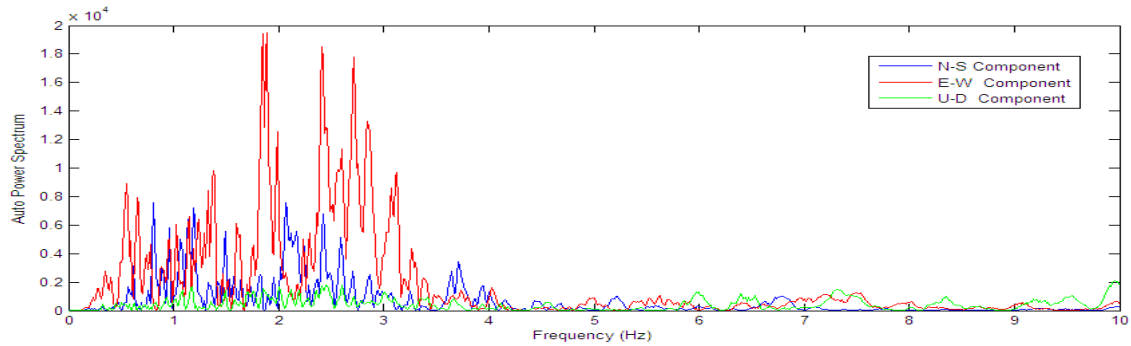


Fig. 8 The autospectrum graphics for all component of the second earthquake between 0-10 Hz

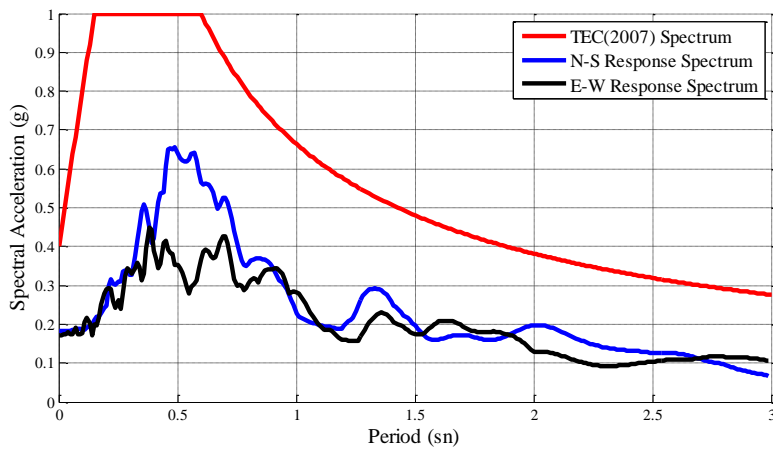


Fig. 9 Ground response spectrum given in Turkish Earthquake Code and calculated response spectrums for North-South and East-West components of the first earthquake with magnitude 6.7

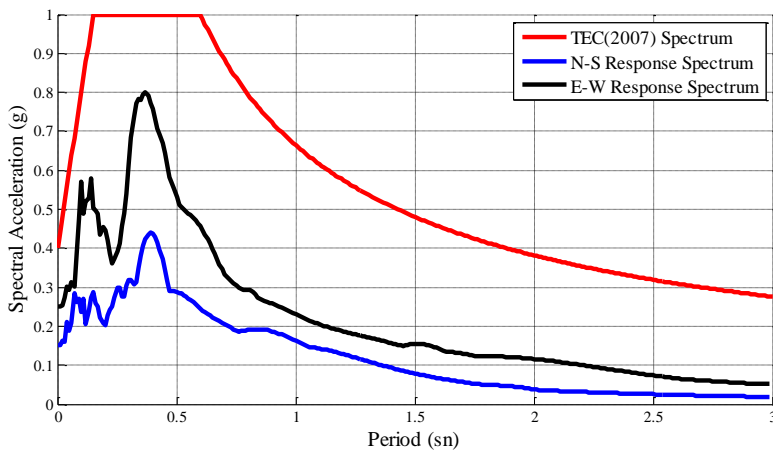


Fig. 10 Ground response spectrum given in Turkish Earthquake Code and calculated response spectrums for North-South and East-West components of the second earthquake with magnitude 5.6

### 3.2 Response spectrums

A response spectrum is obtained by connecting the peak responses of a one degree of freedom system with varying natural frequency under the same base vibration or shock. Response spectrum is very useful tool for analyzing the performance of structures in earthquakes. Firstly, natural frequency of a structure is obtained. After that, the peak response of the building is estimated by determining the value from the ground response spectrum for the appropriate frequency. In most building codes in many country, the response value determined by using response spectrum forms the basis for calculating the forces that a structure must be designed to resist.

In Fig. 9, the ground response spectrum given in Turkish Earthquake Code (TEC) (2007) and calculated response spectrums for North-South and East-West components of the first earthquake with magnitude 6.7 are presented. Similarly, the ground response spectrum given in Turkish Earthquake Code and calculated response spectrums for North-South and East-West components of the second earthquake with magnitude 5.6 are given in Fig. 10. As it can be seen from these figures, the calculated spectrums are lower than the given design spectrum.

As it can be seen in the design spectrums given in Figs. 9-10, the resonance periods of the soil system is between 0.15 sn and 0.60 sn. The frequency values for these periods are 6.66 Hz and 1.67Hz, respectively. The resonant values of calculated autospectrums for north-south and east-west components may be observed between these frequency interval.

## 4. Van train station building subjected to earthquakes

The building consists of three main blocks as shown in Fig. 11. The elevation views of three blocks are given in Fig. 12. The first and third blocks have similar structural systems, however, the second block between these blocks have a different design and structural system. The first and third blocks have three stories and the second block has two stories. In the second block, there is no slab between stories. Therefore, the rigid diaphragm behavior may not be considered in FE modeling for this block.



(a) Direction of the building

(b) General view of all blocks of the building

Fig. 11 The train station building subjected to earthquake effects

### 5. In situ damage assessment of the building due to earthquake effects

When the building is investigated after two main earthquakes and aftershocs, shear failures have been observed over the walls in all blocks as presented in Figs. 13-15. Damage to beam-column joints have been observed in the second block as shown in Fig. 14. The strength of concrete tested after the earthquake is 20 Mpa for first and second block and 10 MPa for the second block. The poor concrete quality and poor detailing despite the requirements of the code causes destruction in the building. On the other hand, there is not a slab between the stories in the second block; therefore the soft-storey effect causes the damages in this block. The soft-storey effect is one of the main contributing factor causing several damages and collapses in multi-storey R/C buildings during the earthquakes. For the second block, the presence of a soft storey resulting with increased deformation has been observed.

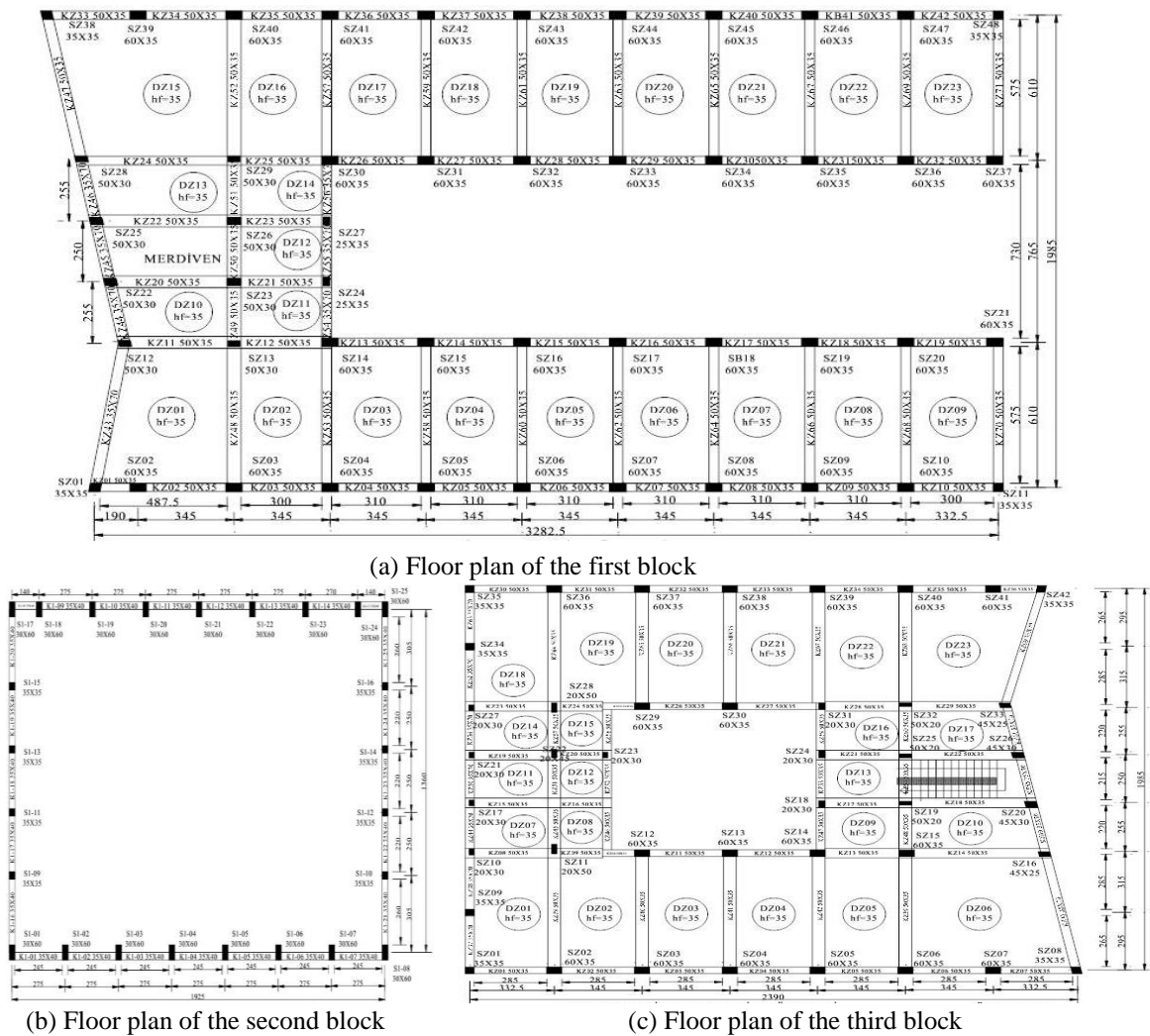


Fig. 12 Floor plans of all blocks of the building



Fig. 13 Damage observations in the first block



Fig. 14 Damage observations in the second block

## 6. Finite element model of the building

With the aim of obtaining more accurate results, 3D finite element models for all blocks was developed based on the geometrical description performed by the in situ observations. Complete



Fig. 15 Damage observations in the third block

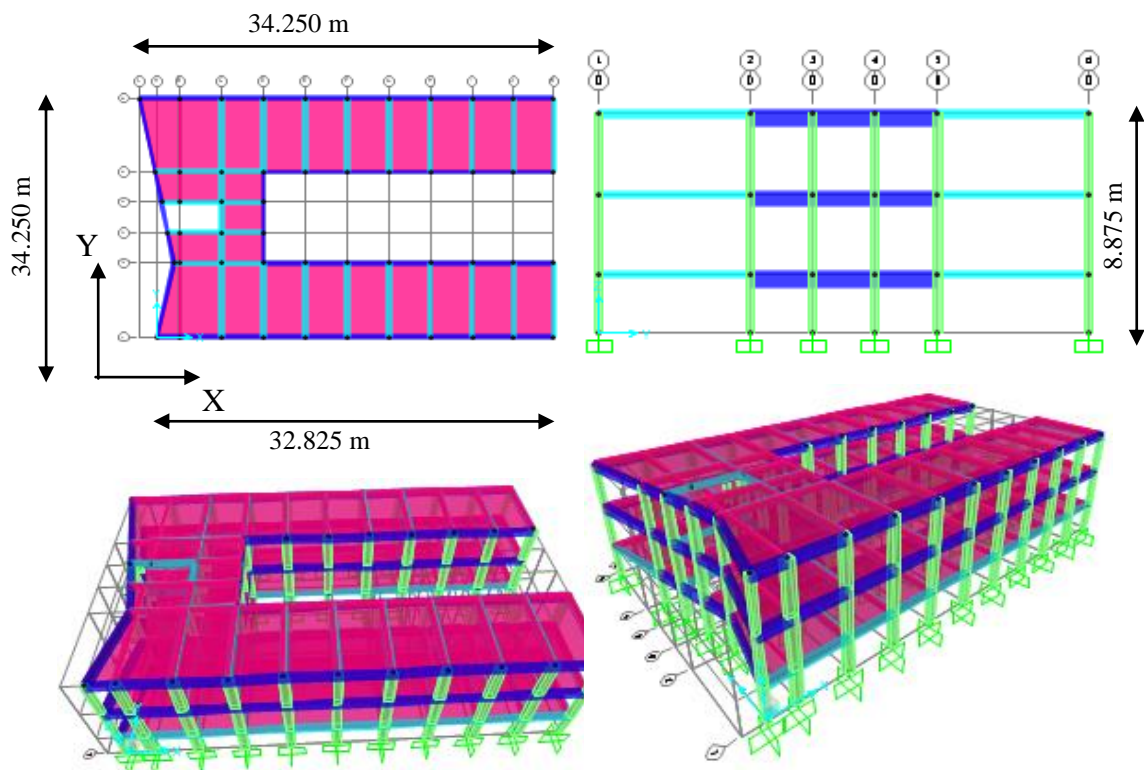


Fig. 16 Finite element model of the first block

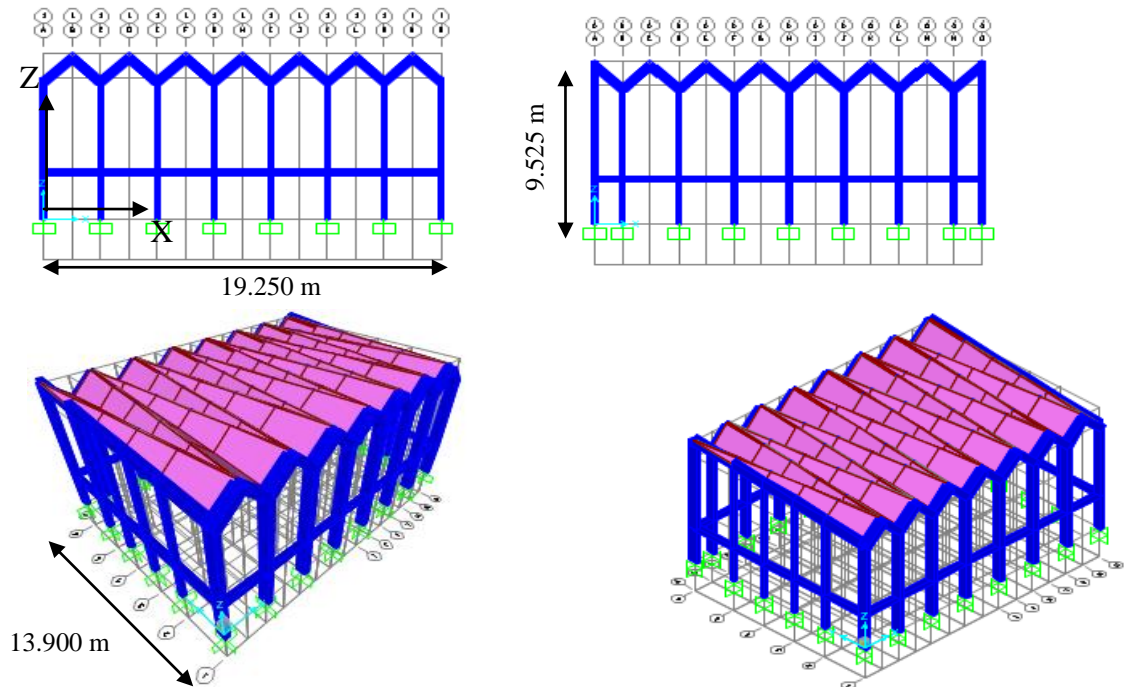


Fig. 17 Finite element model of the second block

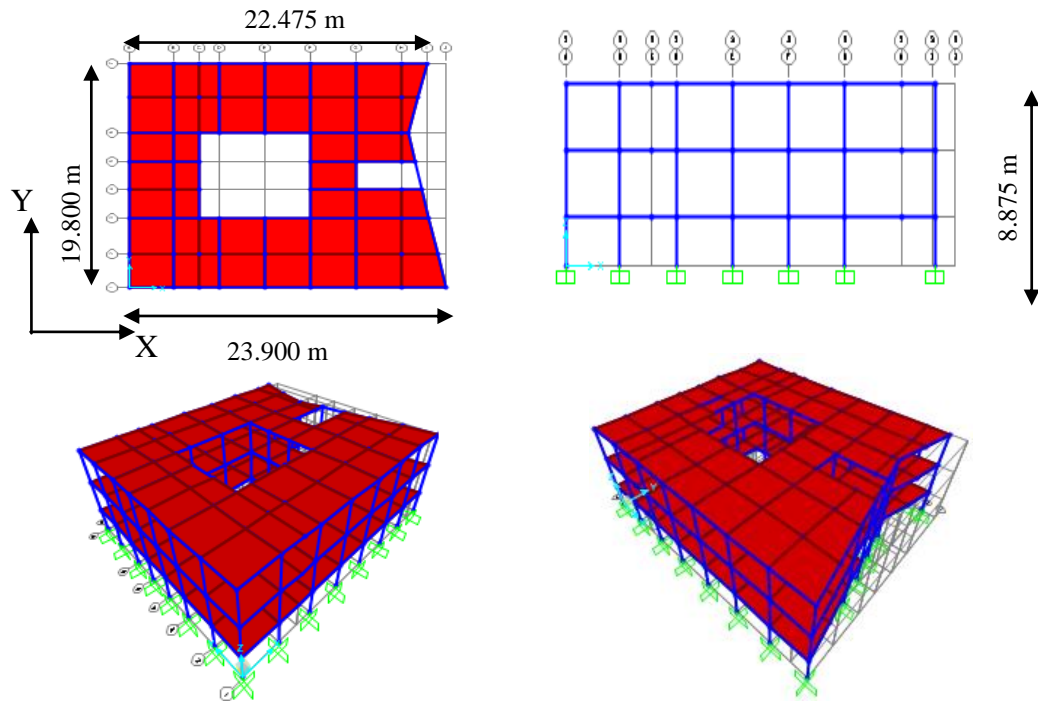


Fig. 18 Finite element model of the third block

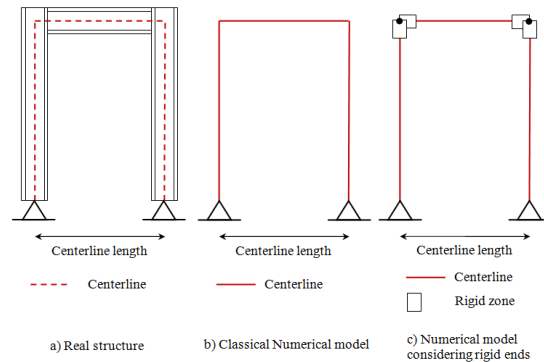


Fig. 19 Real structure, classical model and rigid end model used in FE analysis

three-dimensional FEM models of the blocks have been built using frame and shell elements with SAP2000 analysis program (2009). Figs. 16-18 show the finite element models for all blocks. As it can be seen from Fig. 17, there is not any slab between the stories in the second block and the column length of the second floor is approximately two times of the columns in the first floor. There must be some precautions to increase the lateral rigidity of this block, however, the column dimensions are same and there is not any structural solution to support this weakness in this storey.

### 6.1 Considering rigid-end offsets in structural models

In general FE applications, the centerline dimensions of the real structure are used to create numerical models. Real and the numerical model of a structure in general applications is given in Fig. 19(a) and 19(b). As it can be seen from this figure, the centerline dimensions are used in numerical models and the effect of the joint elements which connects the beams to the columns are assumed to be negligible. However, the effect of the joint element should be checked to obtain a realistic numerical model. Because, in some cases, the stiffness of a joint element may affect the results very much and the assumption may fail.

Rigid-end offsets are used to consider joint elements in structural model. In this simulation technique, the ends of elements are not considered to be part of the flexible portion as shown in Fig. 19(c). With the use of rigid ends in frame elements, the ends of elements are embedded in the connection area with infinite stiffness and more realistic simulation can be carried out.

### 6.2 Seismic analysis by using equivalent static loads

Firstly, equivalent static loads are applied to the classical models and rigid end models. Totally, 18 load combinations are determined and applied to the structural systems. The load combinations are given in Table 1. In the load combinations, the considered loads are as follows:

- Dead load, G
- Live Load, Q
- Equivalent static earthquake load in x direction,  $E_x$
- Equivalent static earthquake load in y direction,  $E_y$

As it can be seen in Table 1, combination 18 consists of all combinations and it gives the extreme results of all. Therefore, the results are evaluated by considering this combination. The

Table 1 Loads combinations used in equivalent static analysis

Load Combinations			
1	1.4G+1.6Q	10	G+Q+Ey+0.3Ex
2	G+Q+Ex+0.3Ey	11	G+Q+Ey-0.3Ex
3	G+Q+Ex-0.3Ey	12	G+Q-Ey+0.3Ex
4	G+Q-Ex+0.3Ey	13	G+Q-Ey-0.3Ex
5	G+Q-Ex-0.3Ey	14	0.9G+Ey+0.3Ex
6	0.9G+Ex+0.3Ey	15	0.9G+Ey-0.3Ex
7	0.9G+Ex-0.3Ey	16	0.9G-Ey+0.3Ex
8	0.9G-Ex+0.3Ey	17	0.9G-Ey-0.3Ex
9	0.9G-Ex-0.3Ey	18	Maksimum(1-17)

Table 2 Equivalent static analysis results for the first block

P (kN)	V <sub>x</sub> (kN)	V <sub>y</sub> (kN)	T (kN-m)	M <sub>y</sub> (kN-m)	M <sub>x</sub> (kN-m)	Drift-x	Drift-y
Basement floor (Rigid End Model)							
-1405.20	-294.21	274.30	-1.62	138.31	148.54	0.00164	0.00371
Basement floor (Classical Model)							
-685.83	-155.05	151.28	-0.78	200.50	206.87	0.00428	0.01112
Ground floor (Rigid End Model)							
-834.20	-277.28	-261.05	2.75	-243.76	-247.45	0.00431	0.00799
Ground floor (Classical Model)							
-316.88	-98.94	-99.10	0.83	-157.84	-154.51	0.00635	0.03331
1st floor (Rigid End Model)							
-267.19	-130.50	129.52	1.51	124.05	-115.54	0.00132	0.00456
1st floor (Classical Model)							
-104.32	-48.35	51.37	0.43	74.96	-70.67	0.00296	0.05833
Base reaction (Rigid End Model)							
8978.51	8377.34	39141.89	391278.88	-598225.04	134310.94		
Base reaction (Classical Model)							
9545.28	9388.11	39141.89	391278.88	-598225.00	164746.32		

obtained results for classical model and rigid end model of the building is given in Tables 2, 3 and 4 for the first, second and third block, respectively.

For evaluating the analysis results effectively, mean values and standard deviations for all columns in each stories are calculated and standard deviations are subtracted from the mean values and obtained results are given to represent the responses of each stories. The base reactions are also given. In these tables, the given structural responses are as follows:

- Axial force, P
- Shear force in x direction, V<sub>x</sub>
- Shear force in y direction, V<sub>y</sub>
- Torsional moment, T
- Bending moment about x direction, M<sub>x</sub>
- Bending moment about y direction, M<sub>y</sub>
- Relative storey drift in x direction, Drift-x
- Relative storey drift in y direction, Drift-y

Table 3 Equivalent static analysis results for the second block

<b>P (kN)</b>	<b>V<sub>x</sub> (kN)</b>	<b>V<sub>y</sub> (kN)</b>	<b>T (kN-m)</b>	<b>M<sub>y</sub> (kN-m)</b>	<b>M<sub>x</sub> (kN-m)</b>	<b>Drift-x</b>	<b>Drift-y</b>
			Ground floor (Rigid End Model)				
-99.92	-25.77	30.98	-0.51	64.90	-32.33	0.0113	0.0097
			Ground floor (Classical Model)				
-101.92	-24.09	30.87	-0.65	61.39	-34.93	0.0132	0.0116
			1st floor (Rigid End Model)				
-71.94	-23.32	26.00	-0.23	-63.20	60.82	0.0482	0.0321
			1st floor (Classical Model)				
-71.63	-21.56	25.86	-0.28	-68.80	61.82	0.0558	0.0390
			Base reaction (Rigid End Model)				
-1354.33	1400.84	3301.42	28627.85	-34336.62	-16290.42		
			Base reaction (Classical Model)				
-1239.05	1404.19	3301.42	28648.19	-33327.69	-16087.87		

Table 4 Equivalent static analysis results for the third block

<b>P (kN)</b>	<b>V<sub>x</sub> (kN)</b>	<b>V<sub>y</sub> (kN)</b>	<b>T (kN-m)</b>	<b>M<sub>y</sub> (kN-m)</b>	<b>M<sub>x</sub> (kN-m)</b>	<b>Drift-x</b>	<b>Drift-y</b>
			Basement floor (Rigid End Model)				
-989.85	177.33	190.34	1.80	99.51	-107.85	-0.0027	0.00319
			Basement floor (Classical Model)				
-1073.05	235.77	236.49	1.69	280.53	-279.04	-0.0063	-0.0128
			Ground floor (Rigid End Model)				
-619.58	173.48	194.07	3.82	-224.64	198.96	-0.0052	0.01051
			Ground floor (Classical Model)				
-650.82	205.71	207.95	2.51	-340.45	335.93	-0.0095	-0.0204
			1st floor (Rigid End Model)				
-209.86	84.20	-97.54	1.56	108.07	-82.99	-0.0019	-0.0308
			1st floor (Classical Model)				
-220.16	100.56	-102.45	1.23	168.02	-164.57	-0.0046	-0.0106
			Base reaction (Rigid End Model)				
5049.46	6219.70	27351.18	269754.92	-311681.68	91009.75		
			Base reaction (Classical Model)				
7013.62	7005.09	27351.18	269754.92	-311681.68	101211.91		

When the analysis results are investigated, the effect of rigid-end offsets may be easily seen. According to the first block analysis results given in Table 2, if rigid ends are taken into account, following differences in the results are obtained;

- The axial forces increases more than two times
- Shear forces in both directions of the building increases about two times
- Moment values decreases about 40% in basement floors and increases about 60% in the ground and the first floor
- Overturning moment (base reaction) in the short direction of the building decreases about 20%
- The relative displacements in the long direction of the building decreases more than two times in the basement and the first floors and %50 in the ground floor.
- The relative displacements in the short direction of the building decreases very much in all the floors.

According to the second block analysis results given in Table 3, if rigid ends are taken into account, following differences in the results are obtained;

- Trivial differences may be observed in element forces
  - The relative displacements in both directions of the building decreases about 20%.
- According to the third block analysis results given in Table 4, if rigid ends are taken into account, following differences in the results are obtained;
- The axial forces are approximately same
  - Shear force in the long direction of the building decreases about 30% in the basement floor and the percentage of diminution goes down 20% towards the first floor
  - Shear force in the short direction of the building decreases about 20% in the basement floor and the percentage of diminution vanishes towards the first floor
  - Moment values decreases about 2.5 times in basement floors and about 60% in the ground and the first floor
  - Overturning moment (base reaction) in the short direction of the building decreases about 10%
  - Axial force as base reaction decreases about 40%
  - The relative displacements in the long direction of the building decreases more than two times in the basement and the first floors and %80 in the ground floor.
  - The relative displacements in the short direction of the building decreases very much in the basement floor, about two times in the ground floor and about 30% in the first floor.

These results may be evaluated more effectively by considering the structural geometry of three blocks. The first blocks has a U shaped slab system along the long direction and there are totally 48 columns in this block. The slab system in third block is more regular and there are totally 42 columns in this block. It means that there is one column per area 9 m<sup>2</sup>. First and third block are similar to each other. The column dimensions and other properties are same, the beams are similar, and the slab systems are same. However, the second block has a different geometry and structural system. This block has a regular geometry and the column lengths in this block are longer than others.

It can be understood from the base reaction results that, the heaviest block is the first block and the biggest shear force effects this block. The lightest block is the second block and the smallest shear force effects this block.

### 6.3 Modal analysis of the building

Modal analysis was performed in order to determine the eigenvalues and eigenmodes of the building. The periods of the first 4 modes are shown in Table 5 and mode shapes are shown in Figs. 20-21. In Table 5, with effect of rigid-end offset, the first periods of the three block of the building change from 0.4629 s to 0.2829 s, 0.6798 s to 0,6056 s, and 0.4993 s to 0.3287 s, respectively. Moreover, the mode shapes basically consist of translation + torsion, torsion + translation, and torsion for all the blocks and vertical oscillation of roof exclusive for the second block.

According to the modal analysis results, if rigid ends are taken into account, following differences in the results are obtained;

- The first natural vibration period decreased 60% in the first block, 10% in the second block and 50% in the third block, respectively.
- The 3rd mode shape in the first block has been changed from translational to torsional.
- The 2nd mode shape in the third block has been changed from torsional to torsional and translational.

Table 5 Modal analysis results containing modal behaviors, periods and modal participation ratios for all degrees of freedom

Mode shape	Mode number	Period (sn)	Modal mass participation ratios					
			UX	UY	UZ	RX	RY	RZ
1st block (Rigid End Model)								
Translation in Y dir. and torsion	1	0.2829	0.0004	0.6829	0.0000	0.1718	0.0000	0.2218
Torsion	2	0.2230	0.0155	0.0227	0.0000	0.0063	0.0015	0.3827
Torsion	3	0.2062	0.0042	0.0006	0.0000	0.0002	0.0005	0.0170
Translation in X dir. and torsion	4	0.1610	0.7457	0.0001	0.0000	0.0000	0.0923	0.1136
1st block (Classical Model)								
Translation in Y dir. and torsion	1	0.4629	0.0000	0.7809	0.0000	0.1778	0.0000	0.3340
Torsion	2	0.3684	0.0004	0.0033	0.0000	0.0008	0.0000	0.2991
Translation in X dir. and torsion	3	0.2828	0.7869	0.0000	0.0000	0.0000	0.0887	0.1529
Translation in X dir. and torsion	4	0.2740	0.0100	0.0000	0.0000	0.0000	0.0011	0.0021
2nd block (Rigid End Model)								
Translation in X dir. and torsion	1	0.6056	0.8111	0.0000	0.0000	0.0000	0.3035	0.1777
Translation in Y dir. and torsion	2	0.4792	0.0000	0.8342	0.0000	0.4251	0.0000	0.3564
Torsion	3	0.4326	0.0002	0.0000	0.0000	0.0000	0.0001	0.2707
Vertical oscillation of roof	4	0.1795	0.0000	0.0000	0.2039	0.0698	0.0957	0.0000
2nd block (Classical Model)								
Translation in X dir. and torsion	1	0.6798	0.8132	0.0000	0.0000	0.0000	0.3038	0.1788
Translation in Y dir. and torsion	2	0.5260	0.0000	0.8362	0.0000	0.4256	0.0000	0.3572
Torsion	3	0.4802	0.0002	0.0000	0.0000	0.0000	0.0001	0.2714
Vertical oscillation of roof	4	0.1842	0.0000	0.0000	0.2080	0.0712	0.0976	0.0000
3rd block (Rigid End Model)								
Translation in Y dir. and torsion	1	0.3287	0.0002	0.6989	0.0000	0.1881	0.0000	0.2989
Torsion and translation in X dir.	2	0.2554	0.3365	0.0012	0.0000	0.0004	0.0676	0.4383
Translation in X dir.	3	0.2047	0.4085	0.0003	0.0000	0.0002	0.0921	0.0036
Translation in Y dir. and torsion	4	0.1054	0.0000	0.0734	0.0010	0.0036	0.0009	0.0353
3rd block (Classical Model)								
Translation in Y dir. and torsion	1	0.4993	0.0000	0.7925	0.0000	0.1926	0.0000	0.3353
Torsion	2	0.3670	0.0406	0.0013	0.0000	0.0005	0.0081	0.3194
Translation in X dir. and torsion	3	0.3434	0.7661	0.0000	0.0000	0.0000	0.1500	0.1434
Translation in Y dir. and torsion	4	0.1752	0.0000	0.0936	0.0000	0.0001	0.0000	0.0449

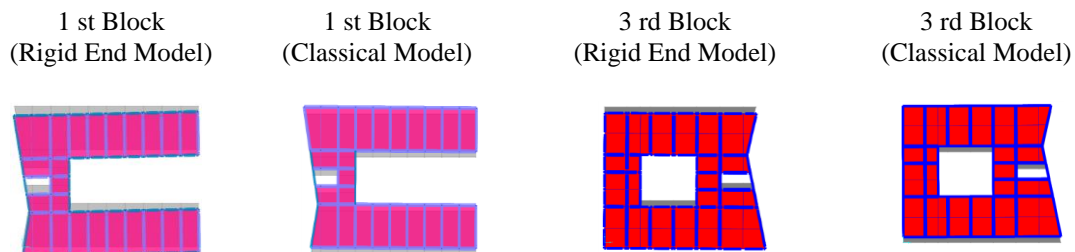


Fig. 20 Modal vectors and natural vibration periods for rigid end model and classical model of first and third block

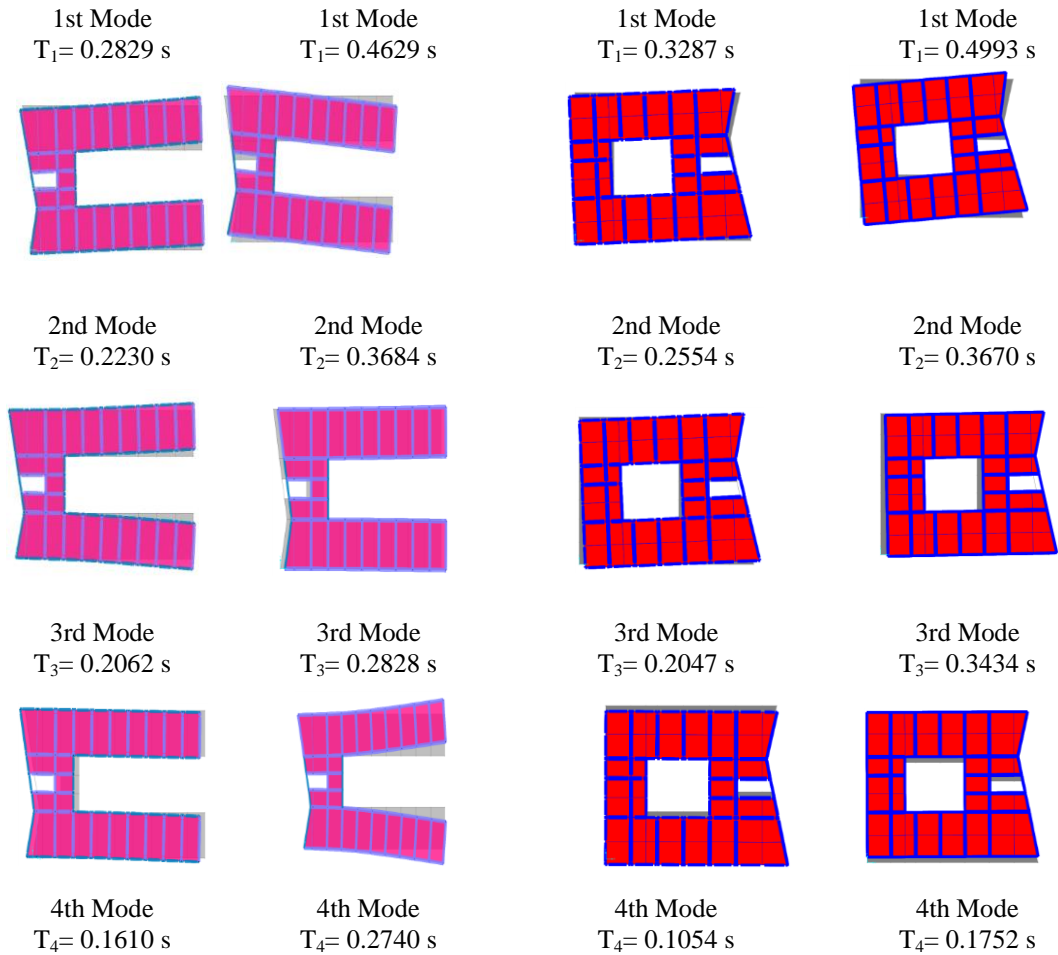


Fig. 20 Continued

#### 6.4 Nonlinear time history analysis of the building

Nonlinear time history analysis is the most effective analysis process for evaluating the proposed methodologies (Yan and Au 2010, Su and Shi 2013) and numerical damage assessments of the historical structures (Bayraktar *et al.* 2010). The earthquake records with magnitude 6.7 and 5.6 obtained from Van Earthquake has been applied to the structure. During the Earthquakes, the second block between the first and third blocks has been damaged because of the striking to other blocks. Therefore, the plastic hinge distribution of this block during the earthquakes will not be evaluated. In this part, the first and third blocks are examined for plastic hinge distribution during the earthquakes. In Table 6, the plastic column and beam ratios are presented for classical and rigid end model of the first block after the earthquakes with magnitude 6.7 and sequential magnitudes 6.7-5.6, respectively. Here, the first earthquake with 6.7 magnitude is applied to the structure and plastic hinge distribution is obtained. After that, the second earthquake with 5.6 magnitude is applied to the structure which have plastic hinges due to first earthquake. The plastic column ratios are given as before collapse and after collapse and totally for classical and rigid end

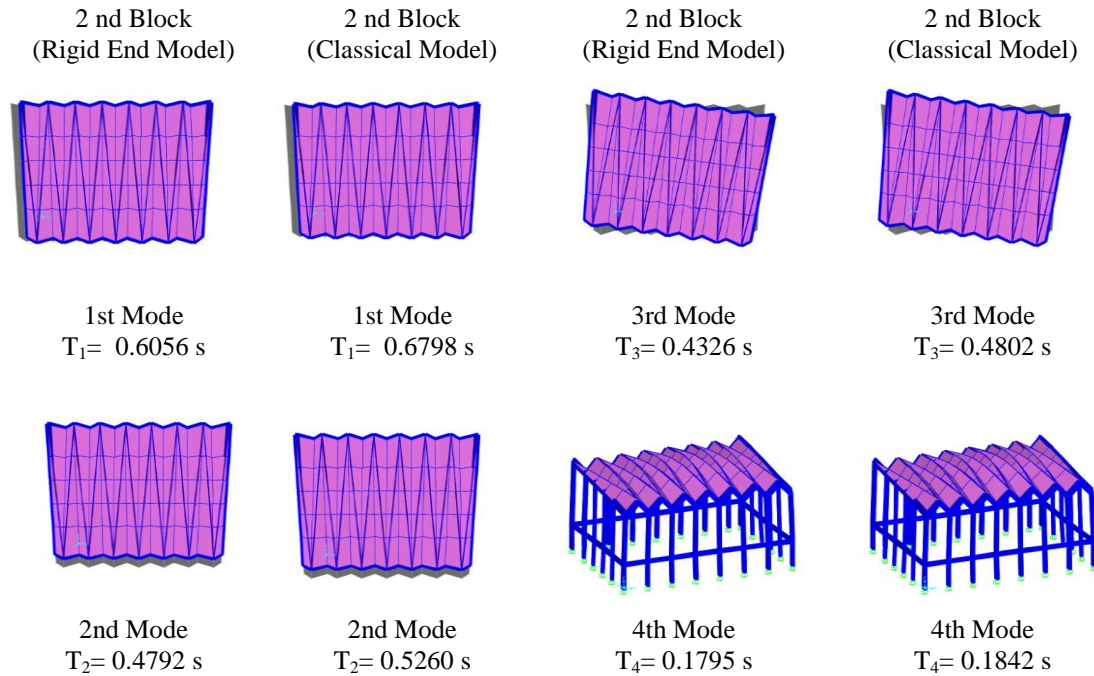


Fig. 21 Modal vectors and natural vibration periods for rigid end model and classical model of the second block

Table 6 Plastic column and beam ratio for classical and rigid end models of the first block after the nonlinear time history analyses

Mg=6.7								
Plastic Column (%)						Plastic Beam (%)		
	Rigid End Model			Classical Model			Rigid End Model	Classical Model
	Before Collapse	After Collapse	Total	Before Collapse	After Collapse	Total	Total	Total
1. Storey	33	0	33	0	50	50	4.5	82
Ground floor	1	49	50	1	49	50	16	75
Basement floor	9	41	50	0	50	50	12	53
Mg=6.7 and 5.6								
Plastic Column (%)						Plastic Beam (%)		
	Rigid End Model			Classical Model			Rigid End Model	Classical Model
	Before Collapse	After Collapse	Total	Before Collapse	After Collapse	Total	Total	Total
1. Storey	75	0	75	25	75	100	6.7	98
Ground floor	1	99	100	1	99	100	43	81
Basement floor	60	39	99	0	100	100	34	66

model. The plastic beam ratios are given totally for both models. Similarly, the plastic column and beam ratios are presented in Table 7 for classical and rigid end model of the third block after the earthquakes with magnitude 6.7 and sequential magnitudes 6.7-5.6, respectively.

Table 7 Plastic column and beam ratio for classical and rigid end models of the third block after the nonlinear time history analyses

Mg=6.7								
	Plastic Column (%)						Plastic Beam (%)	
	Rigid End Model			Classical Model			Rigid End Model	Classical Model
	Before Collapse	After Collapse	Total	Before Collapse	After Collapse	Total	Total	Total
1. Storey	29	26	55	33	11	44	38	18
Ground floor	1	49	50	2	98	100	70	87
Basement floor	23	18	41	32	14	46	63	55

Mg=6.7 ve 5.6								
	Plastic Column (%)						Plastic Beam (%)	
	Rigid End Model			Classical Model			Rigid End Model	Classical Model
	Before Collapse	After Collapse	Total	Before Collapse	After Collapse	Total	Total	Total
1. Storey	40	60	100	66	23	89	53	28
Ground floor	1	49	50	1	99	100	54	68
Basement floor	53	38	91	59	37	96	86	73

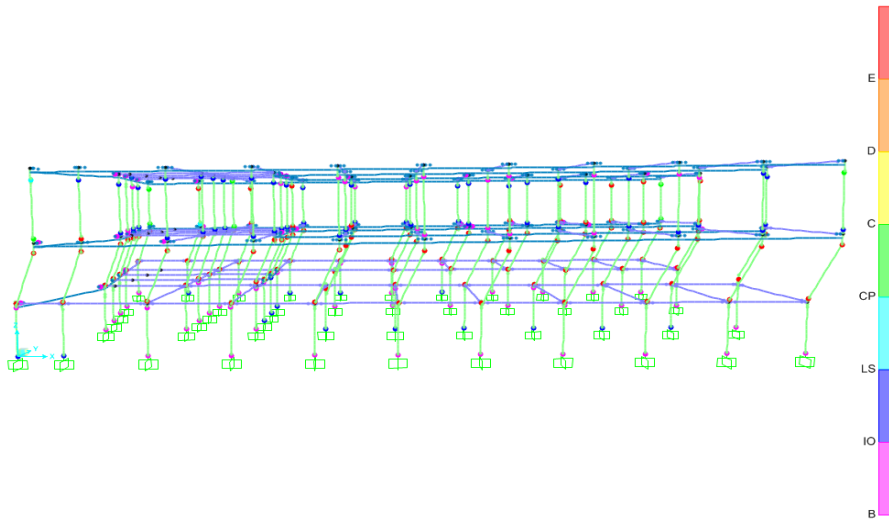
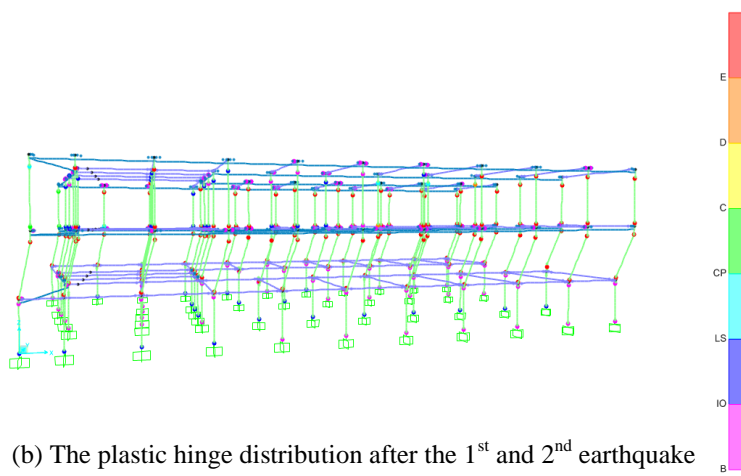
(a) The plastic hinge distribution after the 1<sup>st</sup> earthquake

Fig. 22 The plastic hinge distribution for classical model of the first block after the earthquakes with magnitude 6.7 and sequential magnitudes 6.7-5.6, respectively

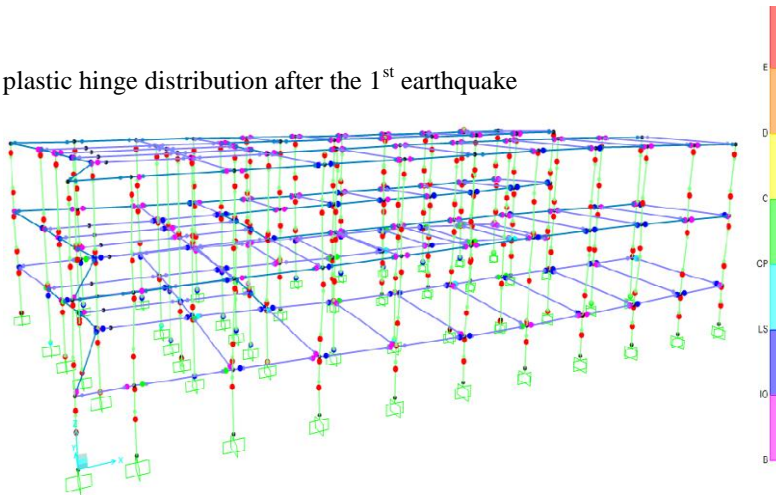
In Fig. 22, the plastic hinge distribution is presented for classical model of the first block after the earthquakes with magnitude 6.7 and sequential magnitudes 6.7-5.6, respectively.



(b) The plastic hinge distribution after the 1<sup>st</sup> and 2<sup>nd</sup> earthquake

Fig. 22 Continued

(a) The plastic hinge distribution after the 1<sup>st</sup> earthquake



(b) The plastic hinge distribution after the 1<sup>st</sup> and 2<sup>nd</sup> earthquake

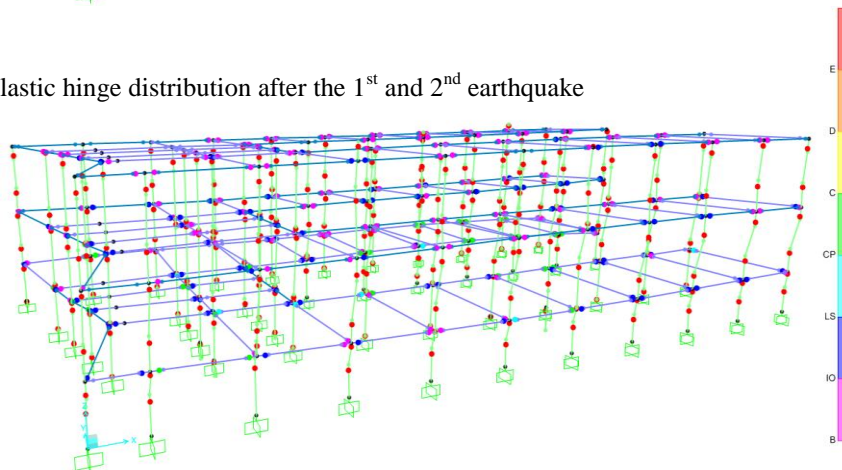


Fig. 23 The plastic hinge distribution for rigid end model of the first block after the earthquakes with magnitude 6.7 and sequential magnitudes 6.7-5.6, respectively

In Fig. 23, the plastic hinge distribution is presented for rigid end model of the first block after the earthquakes with magnitude 6.7 and sequential magnitudes 6.7-5.6, respectively.

According to the nonlinear time history analysis results, if rigid-end offsets are taken into account in the first block, following differences in the results are obtained;

- Total plastic column ratio decreases about 30% in the first story
- Plastic columns after collapse vanishes in the first story
- Plastic columns before collapse appears in the first story
- Total plastic beam ratio decreases significantly in all stories
- In the basement floor, although the total plastic column ratio is same, some of the columns become plastic before collapse

If rigid-end offsets are taken into account in the third block, following differences in the results are obtained;

- In the basement floor, total plastic column ratio decreases about 10% after the first earthquake and 5% after the both earthquakes
- In the ground floor, total plastic column ratio decreases about 50% after the first earthquake and 50% after the both earthquakes
- In the first storey, total plastic column ratio increases about 25% after the first earthquake and increases 10% after the both earthquakes
- Total plastic beam ratio increases about 15% in the basement floor, decreases about 20% in the ground floor and increases about two times in the first storey
- Plastic column ratio decreases before collapse and increases after collapse in the basement floor

## **7. Conclusions**

Numerical damage assessment of a train station affected by Van Earthquake has been carried out for monitoring the effect of rigid-end offsets in framed structures under earthquake excitation. Comparison of results shows that the modeling of structures with rigid-end offsets consistently gives more rigid behavior than that with no rigid-end offsets. In addition, it is found that differences in plastic hinge distribution also exist. Numerically simulated results for analyzing structures with rigid-end offsets were compared with in situ results. These results demonstrated that rigid end models give better results than classical models. The second block between the first and third blocks has been damaged because of the striking to other blocks. Therefore, only first and third blocks have been observed for plastic hinge distribution in analysis process. The analysis results show that it is important to accurately predict the structural responses in capturing the actual behavior of the structure. Finally, significant effects of plastic hinges end offsets on the seismic response are demonstrated.

The observed plastic hinge number over the building due to the both earthquakes is more than the real damage distribution. This situation is due to the following reasons and these effects will be considered in the future parts of this study.

- The walls decrease the lateral displacements of the structure. Therefore, the walls should be considered in numerical models.
- The length of plastic hinges directly effects the plastic hinge formation. The finite element models should be updated to obtain more correct plastic hinge model according to the real structure.

## References

- Tsai, K.C., Wu, S. and Popov, E.P. (1995), "Experimental performance of seismic steel beam-column moment joints", *Journal of Structural Engineering*, **121**(6), 925-931.
- Khudada, A.E. and Geschwindner, L.F. (1997), "Nonlinear dynamic analysis of steel frames by modal superposition", *Journal of Structural Engineering*, **123**(11), 1519-1527.
- Foley, C.M. and Vinnakota, S. (1999), "Inelastic behavior of multistory partially restrained steel frames, Part II", *Journal of Structural Engineering*, **125**(8), 862-869.
- Wong, K.K.F. and Wang, Z. (2007a), "Seismic analysis of inelastic moment-resisting frames Part I: Modified force analogy method for end offsets", *The Structural Design of Tall and Special Buildings*, **16**(3), 267-282.
- Wong, K.K.F. and Wang, Z. (2007b), "Seismic analysis of inelastic moment-resisting frames Part II: Energy dissipation in deformable panel zones", *The Structural Design of Tall and Special Buildings*, **16**(3), 283-299.
- Wong, K.K.F. (2012), "Nonlinear modal analysis of structures with rigid-end offsets", *20th Analysis & Computation Specialty Conference*, ASCE.
- Url1: [http://neic.usgs.gov/neis/eq\\_depot/2011/eq\\_111023\\_b0006bqc/neic\\_b0006bqc\\_w.html](http://neic.usgs.gov/neis/eq_depot/2011/eq_111023_b0006bqc/neic_b0006bqc_w.html), (Accessed October 28, 2012)
- Url 2: Google Maps, <http://maps.google.com/> (Accessed October 28, 2012)
- Heylen, W., Stefan, L. and Sas, P. (2007), *Modal analysis theory and testing*, Katholieke Univ. Leuven, Faculty of Engineering, Dept. of Mechanical Engineering, Leuven, Belgium.
- Şahin, A. and Bayraktar, A. (2010), "SignalCAD: A Digital signal processing software for forced and ambient vibration testing of engineering structures", *J. Test. Eval.*, **38**(1), 95-110.
- MATLAB [Computer software] (2009), Natick, MA, MathWorks.
- Specification for Buildings to be Built in Seismic Zones (2007), Ministry of Public Works and Settlement Government of Republic of Turkey.
- SAP2000 [Computer software] (2009), Integrated Finite Element Analysis and Design of Structures, Computers and Structures Inc., Berkeley, California, USA.
- Yan, Z.H. and Au, F.T.K. (2010), "Nonlinear dynamic analysis of frames with plastic hinges at arbitrary locations", *The Structural Design of Tall and Special Buildings*, **19**(7), 778-801.
- Su, L. and Shi, J. (2013), "Displacement-based earthquake loss assessment methodology for RC frames infilled with masonry panels", *Engineering Structures*, **48**, 430-441.
- Bayraktar, A., Sahin, A., Ozcan, D.M. and Yildirim, F. (2010), "Numerical damage assessment of Haghia Sophia bell tower by nonlinear FE modeling", *Applied Mathematical Modelling*, **34**(1), 92-21.